

Letter

Characterizing streamer branching in N_2-O_2 mixtures by 2D peak-finding

Yuan Li^{1,2} , Siebe Dijcks², Guangyu Sun¹ , Jiaye Wen¹ , Yaoyu Xu¹, Guanjun Zhang¹, Ute Ebert^{2,3} and Sander Nijdam² 

¹ State Key Laboratory of Electrical Insulation and Power Equipment, Xi'an Jiaotong University, Xi'an 710049, People's Republic of China

² Department of Applied Physics, Eindhoven University of Technology, PO Box 513, 5600 MB Eindhoven, The Netherlands

³ Centrum Wiskunde & Informatica (CWI), Amsterdam, The Netherlands

E-mail: gjzhang@xjtu.edu.cn and s.nijdam@tue.nl

Received 7 November 2019, revised 15 January 2020

Accepted for publication 6 February 2020

Published 19 March 2020



Abstract

The stochastic nature of streamers and the manual identification of features in 2D discharge images together cause great ambiguities when analysing streamer branching characteristics. Here we present the development of streamer image diagnostics by a 2D peak-finding method to obtain accurately quantified extensive statistics on streamer branching. And we present quantitative results on the growth of the streamer head number as a function of time in N_2-O_2 mixtures at 100 and 200 mbar. Decreasing the oxygen concentration decreases the nonlocal photoionization, and hence allows for local instabilities and more branching. The oxygen concentration in N_2-O_2 mixtures affects streamer branching not only by smoothening the electron number density in front of streamer heads but also by the creation of an inception cloud. Streamers in pure nitrogen have no noticeable inception cloud, which gives the nitrogen streamers a longer effective propagation time during a voltage pulse of 550 ns; they branch more both as a function of space and of time. However, the statistical results show that the number of streamer heads in high purity N_2 is less than in mixtures with 0.1% O_2 , and it depends on pressure.

Supplementary material for this article is available [online](#)

Keywords: streamer discharge, branching nature, quantified characterization, photoionization

1. Introduction

Streamer discharges typically initiate in a non-uniform, high electric field and can propagate into a region that has a background electric field below the breakdown electric field [1]. Phenomenologically, a streamer is commonly observed as a fast moving head typically of a thin spherical form which propagates forward as an ionization wave and leaves behind an ionized trail [2]. The branching behavior of streamers has been studied in many experiments. During propagation, a streamer channel can split into two [3], three [4] or even more branches [5]. The multiple branching channels are usually

unpredictable and unreproducible leading to an intriguing but very stochastic discharge morphology. The random appearance of streamers both in time and in space has been related to the electron density fluctuations in the lowly ionized region ahead of the streamer head [6, 7]. Branching increases the number of streamer channels, but channels can also die out, thereby reducing the number of active channels.

Streamer branching is one of the fundamental characteristics of discharges. The advance of high-speed imaging techniques and instruments, e.g. intensified charge-coupled devices (ICCD), allows the observation of streamer dynamics on nanosecond or sub-nanosecond timescales. Researchers

can characterize streamer branching by some measurable quantities like channel length and width, velocity, branching angle, etc [8–12]. However, the branching-related parameters extracted and analysed in previous works are generally on an image-by-image basis, which leads to ambiguities due to the very stochastic behavior of streamer discharges under varying applied conditions. Briels *et al* [12, 13] have experimentally measured the branching distance/diameters, propagation velocity of streamers at different pressures in air and pure nitrogen but the data analysis showed large fluctuations although limited images with simple and clear discharge structures were selected before the parameter extraction.

On the other hand, simulation of branching behavior, especially full 3D models, is a very challenging task. Neither one-dimensional nor two-dimensional models can describe streamer branching and interactions; one-dimensional models are restricted to the gap axis, and two-dimensional models treat destabilizing plasma fronts as cones instead of a filamentary branch [14–17]. Furthermore, the experimentally observed branching behavior cannot be fully described numerically if only pure fluid models are used. Very few reported results using particle and hybrid models [6, 7, 18] have shown streamers in 3D to branch.

In one word, although streamer branching has been of great interest to the science community and substantial efforts have been devoted to investigating it, it is still very difficult to quantify branching [12, 13, 19, 20]. In this work, we report our progress on characterizing streamer branching using a 2D peak-finding method. Through automatically processing hundreds of discharge images, we aim to characterize streamer branching in varying N_2 - O_2 mixtures from a big-data perspective: we can acquire extensive statistics on the streamer number and branching characteristics without the human-induced errors in manual counting and tagging.

This work is organized as follows: the experimental setup, applied conditions, and diagnostic methods are treated in section 2. Section 3 presents the experimental results, characterization and analysis of streamer discharges. The summary and conclusions are given in section 4.

2. Experimental arrangement and methodology

Figure 1 illustrates the schematic of the whole experimental setup arrangement. All measurements described here have been performed in a point-plate electrode geometry with 160 mm gap distance inside a vacuum vessel. A detailed description of the vessel can be found in our previous publications [21, 22]. An ICCD camera system (PicoStar HR12) is used for optical diagnostics of the streamer discharge. The ICCD camera is capable of both long exposures as well as (stroboscopic) imaging with gate widths of less than 0.3 ns and can produce images with maximum resolution of 1376×1040 and 12 bit depth of each pixel. The timing system enables the diagnostic system to trigger discharge and camera synchronously. It consists of a programmable timer unit (PTU), a delay generator (2 channels) and a high rate intensifier. This timing system controls the exposure of ICCD

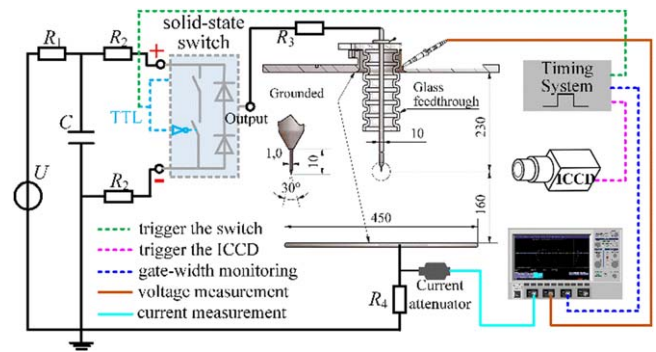


Figure 1. Schematic for the experimental setup arrangement. The DC voltage source can provide up to 60 kV, $R_1 = 20 \text{ M}\Omega$. The charging capacitor $C = 6 \text{ nF}$ (four 1.5 nF parallel capacitors, 40 kV). Together with the switch and the current limitation resistors R_2 , R_3 (of 100 Ω and 25 Ω , respectively), this forms the pulsed voltage. The geometry of the discharge chamber is the same as in [21].

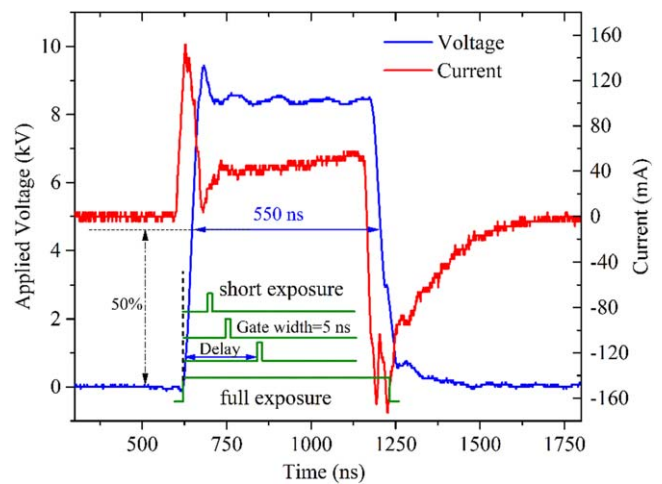


Figure 2. Typical pulsed voltage, current and two kinds of imaging techniques used in the experiments. Full exposure (600 ns gate width) is used to record the entire streamer morphology while serial short exposures (with variable gate width and delay time), are used to record the propagation of streamers and accordingly to calculate the number of streamer branches. The shown example has 8.5 kV voltage, a pulse length of 550 ns and a rise time of 30 ns and is obtained in 100 mbar high purity nitrogen.

and sends out signal to the solid-state switch (Behlke HTS 651-10-GSM) for triggering the HV pulses. The voltage is measured by a high voltage probe (Northstar PVM-4, 1000:1) with a bandwidth of 110 MHz. The current is acquired via a non-inductive resistor of 50 Ohm between cathode and ground, connected to the oscilloscope by an attenuator with a factor of 30 db. The applied pulsed voltage has a frequency of 1 Hz with width of 550 ns and rise time of 30 ns, respectively. A typically employed voltage pulse and ICCD exposure strategies are shown in figure 2.

The background pressure in the vessel can reach as low as 3×10^{-7} mbar. Before the measurement, the leak-rate (including outgassing) of the vessel is tested and found to be 2×10^{-5} mbar min^{-1} . This suggests that the impurity level inside the vessel is less than 50 ppm in total during most measurements (assuming a working pressure of 100 mbar and

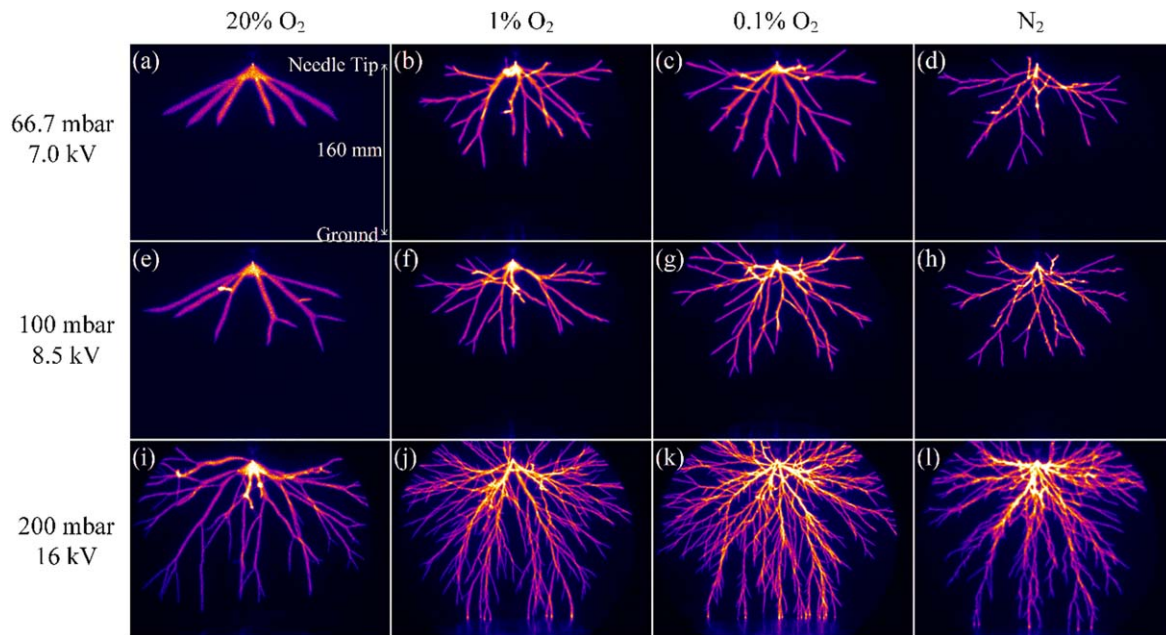


Figure 3. Typical streamer discharge images of 600 ns exposure showing propagation and branching behaviors depending on gas type, gas pressure and excited voltage amplitude. Note that the applied voltage amplitudes are changed according to gas pressures.

an experimental duration of less than 200 min). This is a higher impurity level than in earlier experiments in this vessel due to a recent move of the set-up and the installment of new tubing. The measurements are performed in static gas for a few hours (no gas flow is used).

As the working gases in our experiments, we use four different N_2 - O_2 mixtures, i.e. N_2 - O_2 mixtures with 20%, 1%, 0.1% O_2 concentrations and high purity nitrogen, respectively, aiming to investigate the influences of the N_2 - O_2 mixing ratio on streamer branching characteristics. All working gases are of 6.0 purity, i.e. with less than 1 ppm impurity.

3. Measurement results, characterization and analysis

3.1. Streamer branches measurement by long and short exposures

Typical streamer images of four N_2 - O_2 mixture ratios at varying gas pressures are shown in figure 3. The combinations of voltage amplitude (U) and gas pressure (p) are listed on the left side of figure 3; they are selected such that the ratio U/p between applied voltage and gas pressure is roughly kept constant to get comparable discharge velocities and thereby lengths (for a fixed, short pulse length).

The number and diameter of the branches depend on many parameters including the gas composition, the gas pressure and the applied voltage amplitude [12, 13]. It has been shown in [13] that similarity laws are a reasonable approximation for discharges at different pressures, when U/p is kept fixed. Generally, lower gas pressures (with U/p roughly constant) correspond to broader discharge channels

and less branches, while lower oxygen concentrations lead to more branches, which were already qualitatively known. Streamer branches are distinct and countable when oxygen concentrations are considerably high (e.g. 1%, 20%) and the gas pressure is low (e.g. no more than 100 mbar), as shown in figures 3(a), (b) and (e). We can clearly recognize six branches in figure 3(a). It is also obvious that the streamers in 20% O_2 have much thicker channels than in the other gas mixtures, while for every mixture the channel diameters decrease with increasing gas pressure. Higher gas pressures (densities) do not only shorten the mean free path of particles and decrease the impact ionization time, but also decrease electron attachment time, and hence the decay time of the plasma conductivity. Another property of discharges generated in 20% O_2 is a pronounced inception cloud, a quasi-spherical ionization structure near the electrode tip [23]. The size of the inception cloud decreases for lower oxygen concentrations, related with the nonlocal photoionization [24], until no visible inception cloud appears in pure nitrogen.

The branch counting becomes more and more difficult when streamer channels form more daughter-branches. For lower oxygen concentrations, especially for high purity N_2 (see figure 3(l)), streamers branch more frequently which makes the images quite complex. Some daughter-streamers stem from the main channels, propagate forward and continue to branch; while small daughter-streamers cease to multiply or propagate, which is difficult to identify. In such images, strong luminescence from the main streamer channels makes daughter-branches invisible and the large number of channels inevitably overlay each other. Both reasons make it almost impossible to count the number of streamer branches manually in such images.

Experimental observations [19, 21] and streamer models [16, 25, 26] show that only the propagating head of a streamer

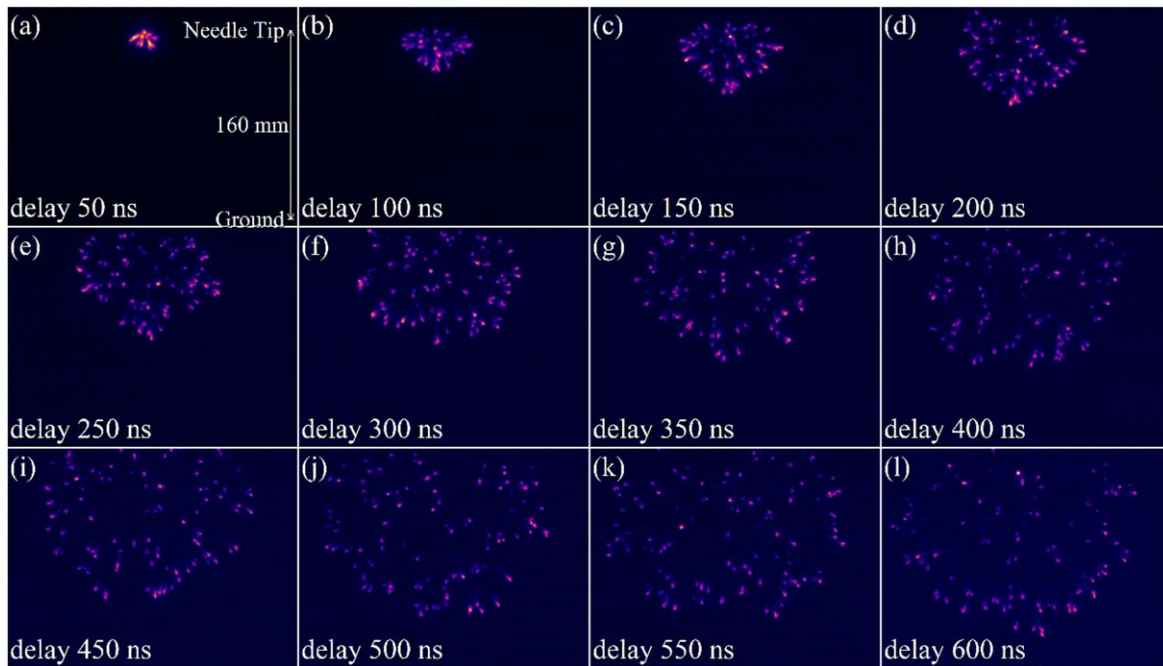


Figure 4. Short (5 ns) exposure images of streamers in 200 mbar N_2 with varying ICCD camera delays. The pulsed voltage amplitude is 16 kV with a width of 550 ns. Note that each panel represents another independent streamer discharge as the ICCD camera can only record one picture per discharge.

channel emits light and an increase of the number of streamer heads therefore indicates the occurrence of branching events. Accordingly, we use short exposures (gate width of 5 ns) to record the streamer heads. We present 5 ns exposure images of streamers in 200 mbar N_2 with varying ICCD camera delays in figure 4.

Streamer heads multiply through repetitive branching during propagation (figures 4(a)–(j)) until the number gets saturated (figures 4(k)–(l)). In this manner, we can quantify streamer branching by finding the number of streamer heads. Therefore, the essence of our method is to find streamer heads or bright dots (i.e. so-called peaks) in hundreds of 2D discharge images.

3.2. Characterizing the number of streamer heads by 2D peak-finding algorithm

Locating and counting the streamer heads (peaks) in such 2D ICCD images is done by image processing. In order to find the peaks in such images accurately, we design a 2D peak-finding algorithm that includes two main procedures. Below, we give a demonstration of this image processing, which is illustrated in figure 5.

Firstly, a 2D spatial bandpass filter is used to suppress pixel noise (or digitization noise) and long-wavelength image variations (e.g. the background brightness) while retaining information of the streamer heads [27]. To achieve this purpose, three steps have been implemented as follows:

- (I) A low-pass image is produced by convolving the original image (see figure 5(a)) with a Gaussian kernel $G(n, \sigma^2)$ in the first place, which suppresses the digitization noise in ICCD and frame grabber. In $G(n,$

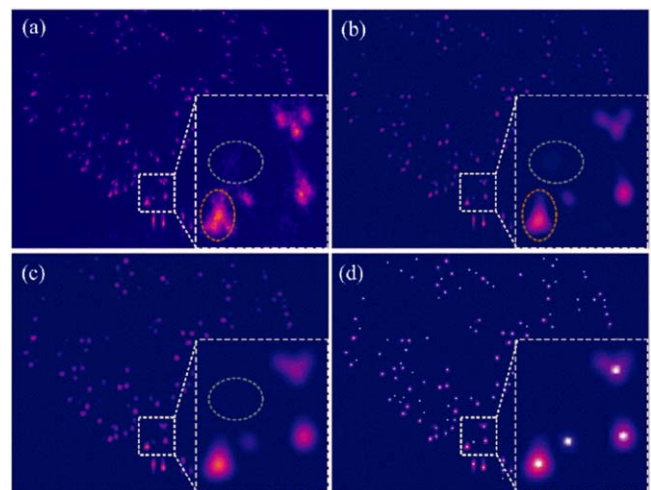


Figure 5. A demonstration of image processing to find and tag streamer heads. Panel (a) shows the original image with 550 ns camera delay, captured in 200 mbar mixture with 0.1% O_2 at 16 kV amplitude. Panel (b) is obtained through processing by a spatial bandpass filter. Panel (c) presents subtracting background noise and strengthening weight of streamer heads and (d) shows the locations of each streamer head found by the local maximum method with a white dot.

σ^2), we use a window of $n \times n$ ($n = 41$ pixels in our algorithm practice) sliding over the original 2D image step by step, and the elements in the window subject to a standard normal distribution, of which the variance is σ^2 ($\sigma = 4$ pixels in our case). The value of σ is crucial to the de-noising but n has less importance. In principle, if σ is assigned large, the digitization noise will be over

suppressed and this will significantly reduce the number of peaks.

(II) We use a boxcar averager [28] (37×37 pixel window) to model the background brightness of the original image. The background brightness would complicate locating streamer heads throughout an entire image. If the window is oversized, the edge distortion of the image cannot be neglected and the total statistic number will be greater than real peaks. However, if the window size is too small, those peaks with weak luminescence will be considered as background brightness and be removed, and thereby number of the peaks will be decreased.

(III) At last, the pre-processed image is obtained by subtracting the boxcar image (Step II) from the Gaussian-filtered image (Step I), as shown in figure 5(b).

The second procedure is to locate and tag each streamer head. In theory, each streamer head can be regarded as a smooth point spread function [29], describing the response of an imaging system to a point source or point object (although a streamer head may be not a complete point source: it has a crescent shape which is elongated by the radiative lifetime). Streamer heads in the image can be determined by finding a peak pixel in an extended blob. During this step, we remove the background noise and employ a convolving operator with another Gaussian kernel $G(21, 6^2)$ to strengthen the weight of each streamer head in an extended blob, which provides a continuous increase of pixel value from zero to a peak (see figure 5(c)). As the value of one pixel only depends on the nearest neighbor pixels in a 2D image [30], we use the local maximum algorithm [31] to locate all the peak pixels (streamer heads) and tag them (see figure 5(d)).

The above-described 2D peak-finding algorithm enables us to calculate the number of branches in an automatic and fast manner for thousands of discharge images with high accuracy. We have identified two possible sources of errors in this method. One is the very low brightness of some streamer heads which can be close to the background noise. The image processing algorithm will remove these potential local peaks (like the gray oval areas in the zoomed frames of figures 5(a) and (c)). The other source of error may originate from the overlapping projection of two or more streamer heads to a 2D image. Such overlap may be smoothed out by our algorithm and hence can be tagged as one head (see the differences between the red oval areas in the zoomed frames of figures 5(a) and (b)). Consequently, due to the two above points, the number of streamer heads obtained by our 2D peak-finding method may be lower than the real number.

3.3. Influence of N_2 - O_2 concentration on branching: analysis and discussion

We have employed the above-described 2D peak-finding algorithm to automatically calculate the streamer heads number. Figure 6 plots the streamer head number as a function of camera delay time in varying N_2 - O_2 mixtures at 100

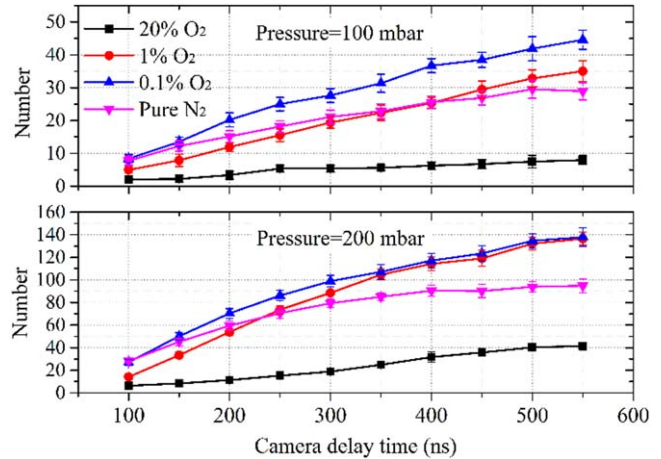


Figure 6. The streamer head number as a function of camera delay time in varying N_2 - O_2 mixtures at 100 mbar (8.5 kV voltage amplitude) and 200 mbar pressure (16 kV voltage amplitude), respectively.

and 200 mbar. All the data points shown in this paper are averages from 100 separate discharge images for each condition and are plotted with their standard deviation.

The figure shows that 100 ns after the voltage pulse has started, the streamers have begun to branch. The number of branches in 100 mbar artificial air (20% O_2 mixture) is less than 10 while this number is 44.5 ± 3 in the 0.1% O_2 mixture for the same conditions. When the voltage amplitude is increased to 16 kV and the pressure to 200 mbar in N_2 - O_2 mixtures, the streamer channels propagate further and branch much more frequently than their 100 mbar counterparts do. Taking 0.1% O_2 mixture for instance, the number of branches at $t = 500$ ns is around 140 at 200 mbar, while this number is only 41.8 at 100 mbar.

It is clear that the streamer head number in artificial air under both pressures is far less than in other mixtures with low oxygen concentration. It can be explained by the fact that the discharges in artificial air have a pronounced inception cloud and that the streamers will not start to really propagate and then form possible branches until the inception cloud breaks up. This has been shown in our previous work [22, 23] in which we used a fixed exposure time and a varying delay time of the camera exposure to determine when the streamers exactly start and when they branch (or also see supplementary figure S1, which is available online at stacks.iop.org/PSST/29/03LT02/mmedia).

It can be generally concluded that for lower oxygen concentrations or higher gas pressure streamers branch more, something which was already qualitatively known [21, 32] but was never quantified before. This is explained by photoionization [33, 34], which is abundant in air but rare in pure nitrogen. This effect smoothens the electron number density in front of propagating streamers and hence reduces local instabilities, thereby mitigating branching.

If we go further with this understanding, it can be speculated that streamers in pure N_2 would branch most among the different mixtures as photoionization plays only a minor role (considering the impurity level inside the vessel).

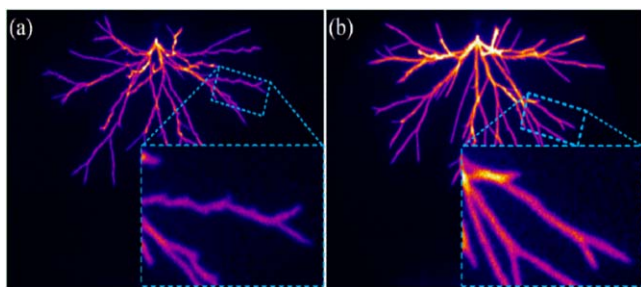


Figure 7. Streamer morphologies in (a) pure N_2 and (b) 0.1% O_2 at 100 mbar including a detailed comparison of streamer channels.

However, it is surprising to find that streamers in pure N_2 have fewer channels than mixtures with 0.1% O_2 at both gas pressures. In order to understand this, we compare streamer morphologies in pure N_2 and 0.1% O_2 mixture at 100 mbar in figure 7. In pure N_2 , the streamer channels elongate crookedly (see the zoomed area in panel 7(a)), while the branches in 0.1% O_2 are thicker and straighter (panel 7(b)). The bending points on the crooked channels, also called feathery structures [5, 21], are likely attempts at new daughter-branches, but a counter mechanism may play a competitive role that prevents these tiny branches to grow into real branches. Wormeester *et al* [35] found that sufficiently low background electron density as well as sufficiently high electric field ahead of the main channel both enable the formation of distinct avalanches moving towards the streamer heads and hence the formation of the tiny, but optically distinguishable branches. These tiny branches observed through the long exposure are either invisible or too dim in the 5 ns short exposures and may be removed by the filtering procedures (see figures 5(a) and (c)).

4. Summary and conclusions

We report our progress on characterizing streamer branching in N_2 – O_2 mixtures by using short ICCD camera exposures and a 2D image peak-finding diagnostic method. In this manner, we quantify streamer branching by finding the number of streamer heads and we can acquire extensive statistics on the streamer number and branching characteristics without the human-induced errors in manual counting and tagging. This image-processing algorithm can greatly facilitate processing of time-resolved measurements of streamer propagation and enhances streamer branching characterization.

The experimental results in four different N_2 – O_2 mixtures quantitatively show that streamers tend to branch more at lower oxygen concentration due to decreasing photo-ionization. The oxygen concentration in the N_2 – O_2 mixtures can influence streamer branching not only by smoothing the electron number density in front of streamer heads but also due to the formation of an inception cloud, especially in artificial air (20% O_2). When the inception cloud breaks up, streamers start to grow and then to branch. Streamers in nitrogen have no noticeable inception cloud, so they have more effective propagation time during the voltage pulse and





hence propagate further. It has been verified by our previous experimental work [22] that the streamers in high purity N_2 start to branch much earlier in time (at least 60 ns at 66.7 mbar under 7 kV) and longer distance in space (~ 10 mm from the needle tip) than in air at the same pressure.

It is surprising to find that the number of branches in pure N_2 is significantly lower than in 0.1% O_2 at the conditions. This can be explained through microscopic comparisons of branches that many tiny streamer branches in pure N_2 fail to grow into real branches and are therefore not counted in the short exposure images. The stochasticity induced by the low photo-ionization density may explain the occurrence of those many small branches, but a possible counter mechanism must exist which suppresses the tiny branches to grow into real branches.

Acknowledgments

This work was supported by National Natural Science Foundation of China (51607139).

ORCID iDs

Yuan Li  <https://orcid.org/0000-0001-5424-1764>
 Guangyu Sun  <https://orcid.org/0000-0001-6761-6019>
 Jiaye Wen  <https://orcid.org/0000-0001-8160-5148>
 Sander Nijdam  <https://orcid.org/0000-0002-1310-6942>

References

- [1] Raizer Y P 1991 *Gas Discharge Physics* (Berlin: Springer)
- [2] Lagarkov A N and Rutkevich I M 2012 *Ionization Waves in Electrical Breakdown of Gases* (New York: Springer Science & Business Media)
- [3] Teramoto Y, Fukumoto Y, Ono R and Oda T 2011 Streamer propagation of positive and negative pulsed corona discharges in air *IEEE Trans. Plasma Sci.* **39** 2218–9
- [4] Heijmans L C J, Nijdam S, Veldhuizen E M van and Ebert U 2013 Streamers in air splitting into three branches *Europhys. Lett.* **103** 25002
- [5] Heijmans L C J, Clevis T T J, Nijdam S, van Veldhuizen E M and Ebert U 2015 Streamer knotwilg branching: sudden transition in morphology of positive streamers in high-purity nitrogen *J. Phys. D: Appl. Phys.* **48** 355202
- [6] Luque A and Ebert U 2011 Electron density fluctuations accelerate the branching of positive streamer discharges in air *Phys. Rev. E* **84** 046411
- [7] Bagheri B and Teunissen J 2019 The effect of the stochasticity of photoionization on 3D streamer simulations *Plasma Sources Sci. Technol.* **28** 045013
- [8] Stenbaek-Nielsen H C and McHarg M G 2008 High time-resolution sprite imaging: observations and implications *J. Phys. D: Appl. Phys.* **41** 234009
- [9] Kanmae T, Stenbaek-Nielsen H C, McHarg M G and Haaland R K 2012 Diameter-speed relation of sprite streamers *J. Phys. D: Appl. Phys.* **45** 275203

- [10] Gerken E A, Inan U S and Barrington-Leigh C P 2000 Telescopic imaging of sprites *Geophys. Res. Lett.* **27** 2637–40
- [11] Chen S, Wang F and Sun Q 2018 The branching characteristics of positive streamers in nitrogen-oxygen gas mixtures *IEEE Trans. Dielectr. Electr. Insul.* **25** 1128–34
- [12] Briels T M P, Kos J, Winands G J J, Veldhuizen E M van and Ebert U 2008 Positive and negative streamers in ambient air: measuring diameter, velocity and dissipated energy *J. Phys. D: Appl. Phys.* **41** 234004
- [13] Briels T M P, Veldhuizen E M van and Ebert U 2008 Positive streamers in air and nitrogen of varying density: experiments on similarity laws *J. Phys. D: Appl. Phys.* **41** 234008
- [14] Grange F, Soulem N, Loiseau J F and Spyrou N 1995 Numerical and experimental determination of ionizing front velocity in a DC point-to-plane corona discharge *J. Phys. D: Appl. Phys.* **28** 1619–29
- [15] Tardiveau P, Marode E and Agneray A 2002 Tracking an individual streamer branch among others in a pulsed induced discharge *J. Phys. D: Appl. Phys.* **35** 2823
- [16] Xiong Z and Kushner M J 2014 Branching and path-deviation of positive streamers resulting from statistical photon transport *Plasma Sources Sci. Technol.* **23** 065041
- [17] Babaeva N Y, Naidis G V, Tereshonok D V and Son E E 2018 Development of nanosecond discharges in atmospheric pressure air: two competing mechanisms of precursor electrons production *J. Phys. D: Appl. Phys.* **51** 434002
- [18] Li C, Teunissen J, Nool M, Hundsdorfer W and Ebert U 2012 A comparison of 3D particle, fluid and hybrid simulations for negative streamers *Plasma Sources Sci. Technol.* **21** 055019
- [19] Lu X and Ostrikov K 2018 Guided ionization waves: The physics of repeatability *Appl. Phys. Rev.* **5** 031102
- [20] Popov N A 2002 Spatial structure of the branching streamer channels in a corona discharge *Plasma Phys. Rep.* **28** 615–22
- [21] Nijdam S, Wetering F M J H, van de, Blanc R, Veldhuizen E M van and Ebert U 2010 Probing photoionization: experiments on positive streamers in pure gases and mixtures *J. Phys. D: Appl. Phys.* **43** 145204
- [22] Li Y, van Veldhuizen E M, Zhang G J, Ebert U and Nijdam S 2018 Positive double-pulse streamers: how pulse-to-pulse delay influences initiation and propagation of subsequent discharges *Plasma Sources Sci. Technol.* **27** 125003
- [23] Chen S, Heijmans L C J, Zeng R, Nijdam S and Ebert U 2015 Nanosecond repetitively pulsed discharges in N_2-O_2 mixtures: inception cloud and streamer emergence *J. Phys. D: Appl. Phys.* **48** 175201
- [24] Teunissen J and Ebert U 2016 3D PIC-MCC simulations of discharge inception around a sharp anode in nitrogen/oxygen mixtures *Plasma Sources Sci. Technol.* **25** 044005
- [25] Pancheshnyi S V, Starikovskaia S M and Starikovskii A Y 2001 Role of photoionization processes in propagation of cathode-directed streamer *J. Phys. D: Appl. Phys.* **34** 105
- [26] Ningyu L and Pasko Victor P 2004 Effects of photoionization on propagation and branching of positive and negative streamers in sprites *J. Geophys. Res.-Space* **109** A01301
- [27] Crocker J C and Grier D G 1996 Methods of digital video microscopy for colloidal studies *J. Colloid Interfaces Sci.* **179** 298–310
- [28] Kotov I V, Kotov A I, Frank J, Kubanek P, O'Connor P, Radeka V and Takacs P 2011 Lateral diffusion estimation in fully depleted thick CCD using flat field image analysis *Nucl. Instrum. Methods Phys. Res. A* **652** 524–7
- [29] Breckinridge J B, Lam W S T and Chipman R A 2015 Polarization aberrations in astronomical telescopes: the point spread function *Publ. Astron. Soc. Pac.* **127** 445–68
- [30] Li S Z 2009 *Markov Random Field Modeling in Image Analysis* (London: Springer)
- [31] Zhang S X, Xing M D, Xia X G, Liu Y Y, Guo R and Bao Z 2013 A robust channel-calibration algorithm for multi-channel in azimuth HRWS SAR imaging based on local maximum-likelihood weighted minimum entropy *IEEE Trans. Image Process.* **22** 5294–305
- [32] Nudnova M M and Yu S A 2008 Development of streamer flash initiated by HV pulse with nanosecond rise time *IEEE Trans. Plasma Sci.* **36** 896–7
- [33] Naidis G V 2018 Effects of photoionization characteristics on parameters of positive streamers *Plasma Res. Express* **1** 017001
- [34] Pancheshnyi S 2015 Photoionization produced by low-current discharges in O_2 , air, N_2 and CO_2 *Plasma Sources Sci. Technol.* **24** 015023
- [35] Wormeester G, Nijdam S and Ebert U 2011 Feather-like structures in positive streamers interpreted as electron avalanches *Japan. J. Phys. D: Appl. Phys.* **50** 08JA01

Supplementary Material

Characterizing streamer branching in N₂-O₂ mixtures by 2D peak-finding

Yuan Li^{1, 2}, Siebe Dijcks², Guangyu Sun¹, Jiaye Wen¹, Yaoyu Xu¹, Guanjun Zhang^{1 a)}, Ute Ebert^{2, 3} and Sander Nijdam^{2 b)}

¹ State Key Laboratory of Electrical Insulation and Power Equipment, Xi'an Jiaotong University, Xi'an 710049, P.R. China

² Department of Applied Physics, Eindhoven University of Technology, PO Box 513, 5600 MB Eindhoven, The Netherlands

³ Centrum Wiskunde & Informatica (CWI), Amsterdam, The Netherlands

E-mail: ^{a)} gjzhang@xjtu.edu.cn and ^{b)} s.nijdam@tue.nl

On the inception stage for artificial air (20% O₂) and pure N₂

We use a fixed exposure time (30ns) and a varying delay time of the camera exposure to determine when the streamers exactly start and when they branch. The morphology of streamers at the inception stage in artificial air (20% O₂) and pure N₂ for two pressures with varying camera delay times is shown in Fig. S1. The results show that in artificial air, a pronounced inception cloud causes the branching to occur later than in nitrogen. According to Fig. S1 (a)-(e) and (f)-(j), the inception cloud in air experiences a series of shape changes, from a spherical cloud to a growing shell and a flat shell (with destabilization on the shell edge) before it eventually breaks up into multiple streamer channels. The inception cloud in 100 mbar air breaks up at 150 ns and starts to branch at 200 ns, while at 16 kV in 200 mbar air, the inception cloud breaks up at 90 ns and starts to branch at about 120 ns (see Fig. S1 (j)). Streamers in nitrogen have no noticeable inception cloud (see Fig. S1 (k)-(t)) and start to propagate much earlier in the voltage pulse. Therefore, they have real branches much earlier than streamers in air.

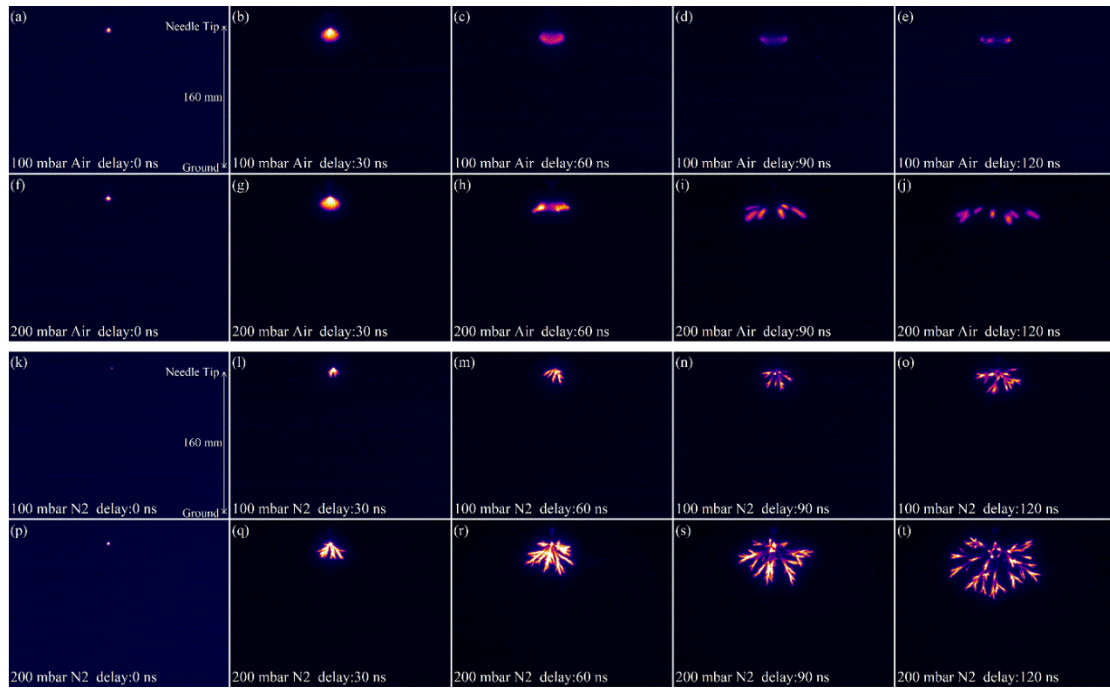


Fig. S1. The morphology of streamers at the inception stage for artificial air (20% O_2) and pure N_2 for two pressures for varying camera delays. Artificial air: 100 mbar (a-e) and 200 mbar (f-j); Nitrogen: 100 mbar (k-o) and 200 mbar (p-t). The gate width for capturing each image is 30 ns